# MODELLING OF HTRs WITH MONTE CARLO: FROM A HOMOGENEOUS TO AN EXACT HETEROGENEOUS CORE WITH MICROPARTICLES

**Rita PLUKIENE[a,b] and Danas RIDIKAS [a] [1]**

[a])DSM/DAPNIA/SPhN, CEA Saclay, F-91191 Gif-sur-Yvette, France
[b])Institute of Physics, Savanoriu 231, LT-2600 Vilnius, Lithuania

## ABSTRACT

The gas turbine modular helium-cooled reactor (GT-MHR) is known probably as the best option for the maximum plutonium destruction in once-through cycle, even though the industrial fabrication of coated particle fuel still has to be proved. We perform detailed Monte Carlo simulations along these lines by comparing different geometry sets, namely homogeneous versus single-heterogeneous and double-heterogeneous, in terms of $k_{eff}$ eigenvalues, the length of the fuel cycle, neutron characteristics and the evolution of fuel composition in particular. In all cases the same Monteburns code system is used. We show that the performance of GT-MHR may be considerably influenced by the way its geometry is modelled within the Monte Carlo approach.

## 1. INTRODUCTION

Gas-cooled reactor technologies (e.g. GT-MHR [1]) seem to offer significant advantages in accomplishing the transmutation of plutonium isotopes and nearly total destruction of $^{239}$Pu in particular. GT-MHR uses a variable in time neutron spectrum, operates at high temperature and employs ceramic-coated fuel. It utilises natural erbium as a non-fertile burn-able poison with the capture cross section having a resonance at a neutron energy such that ensures a strong negative temperature coefficient of reactivity. The lack of interaction of neutrons with coolant (helium gas) makes sure that temperature feedback is the only significant contributor to the power coefficient. As a matter of fact, no additional plutonium is produced since no $^{238}$U is used. A gas-cooled high temperature reactor or a separate irradiation zone in the centre of GT-MHR assembly, coupled to an accelerator [2], could also provide a fast neutron environment due to the same reason -- the helium coolant is essentially transparent to neutrons and does not change neutron energies. Since other actinides with an exception of plutonium are more inclined to fission in a fast neutron energy spectrum, one could consider an additional fast stage, following a thermal stage, in order to eliminate the remaining actinides [2].

In this paper we will describe in detail the use of a critical GT-MHR for transmutation of Pu isotopes from military applications. We note separately that a similar study with civil plutonium as a fuel has also been carried out but to be reported elsewhere due to a limited size of this manuscript. The main goal of our study is to compare the performance parameters of the reactor core in the once-through cycle as a function of different geometry representation, i.e. homogeneous, single-heterogeneous and double-heterogeneous within Monte Carlo approach. Monteburns [3], namely a coupled MCNP [4] and ORIGEN [5] code system, is employed at different stages of our simulations. The performance of it has been successfully benchmarked in Ref. [6] by simulating the fuel cycle of the high flux reactor

---

of ILL Grenoble (France). We note that our preliminary results on the homogeneous versus single-heterogeneous GT-MHR with Monte Carlo were already reported in part in Ref.[7], and also addressed in part in Ref. [8] but with different modelling schemes, e.g. a deterministic approach and/or based on the neutron diffusion theory.

## 2. MODELLING PROCEDURE

A simplified 3D model of GT-MHR reactor, which is shown in Fig. 1A, has been created using the MCNP geometry set-up. Further details on this homogeneous geometry modelling including some burn-up calculations can be found in [9]. We also refer the reader to Refs. [10,11], where a comparative analysis of different data libraries and corresponding influence on the performance of a homogeneous GT-MHR has already been reported.



|        |        | $\Phi_{therm}$, % |        |        |
|--------|--------|--------|--------|
|        |        | HTR 1  | HTR 2  | HTR 3  |
| 0 d    |        | 10.0   | 9.6    | 11.0   |
| 200 d  |        | 11.6   | 10.7   | 12.3   |
| 400 d  |        | 15.2   | 13.1   | 14.8   |
| 600 d  |        | 20.9   | 17.8   | 18.8[*]|
| 800 d  |        | 32.9   | 28.8   |        |

(A)          (B)
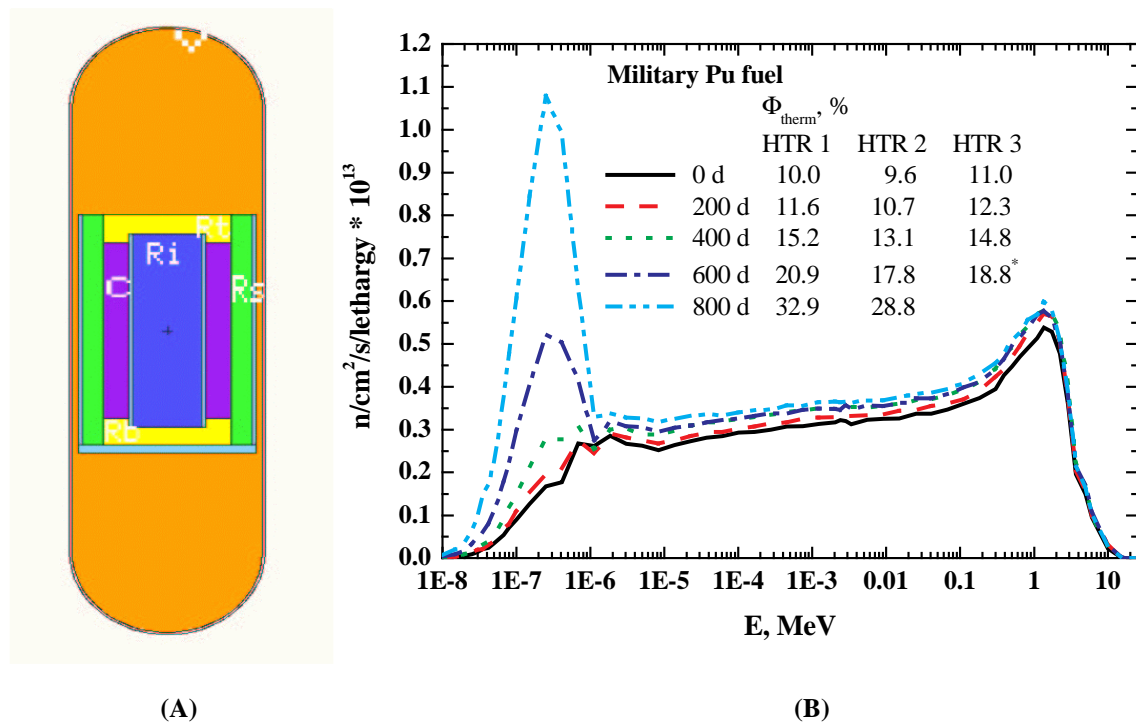
**Figure 1: A)** Length-wise section view of GT-MHR reactor model. The following notation is employed: C – active core (~8 m high), Rt - top reflector, Ri – inner reflector, Rb - bottom reflector, Rs - side reflector, and V - reactor vessel. **B)** Typical change of the average energy spectra of neutrons in the active core of GT-MHR for different fuel burn-up expressed in full power days. The thermal neutron contribution are presented in a table for each geometry configuration. [*] Note that the fuel cycle of HTR3 ends after 550 days.

In this work we also used MCNP to obtain k-eigenvalues and neutron fluxes. As soon as $k_{eff} < 1$ the length of the fuel cycle is determined in the case of a critical system. A typical neutron spectrum evolution for Pu fuel poisoned with natural Er is shown in Fig. 1B. The observed increase of the thermal flux from 10% to 30% is due to the loss of $^{239}$Pu and $^{240}$Pu in addition to the loss of the burn-able poison during the operation for different geometry cases. Indeed, the change of the energy spectra of neutrons will change the average cross sections to be used in the burn-up calculations, in some cases by a factor of two or more [9]. Therefore fuel evolution calculations have to be performed with corresponding variable neutron fluxes as it is done with Monteburns [3]. We note also that at the constant reactor power typical averaged GT-MHR neutron fluxes in the active core may increase

typically by 50-100 %, i.e. from ~1×10$^{14}$ n/(cm$^2$ s) to ~2×10$^{14}$ n/(cm$^2$ s) at the beginning and at the end of the fuel cycle respectively [9].

## 3. HOMOGENEOUS AND HETEROGENEOUS GT-MHR

### 3.1. MAJOR GEOMETRY AND MATERIAL CHARACTERISTICS

As it was mentioned above, our major interest in this study was to look at the GT-MHR performance parameters by investigating three different geometry configurations: homogeneous (HTR1), single-heterogeneous (HTR2) and double-heterogeneous (HTR3).

The cross sectional view of the first type geometry HTR1, is presented in Fig. 2A. It includes hexagonal lattice structure with all material compositions distributed homogeneously over corresponding zones and characterised by specific material densities. An active core consists of 102 hexagonal prism columns located around the inner reflector (37 columns) in addition to a separate zone with $B_4C$ (24 columns). Side replaceable and permanent graphite reflectors are constructed similarly around the active core.

A single-heterogeneous geometry's (HTR2) feature is an explicit active core structure (see Fig. 3A.). In this case each hexagonal core column consists of 202 cylinders with fuel material, 14 cylinders with natural erbium and 108 cylinders with helium as it is shown in Fig. 3B. Fuel and erbium materials are homogeneously placed in the silicon – graphite matrix in the form of homogenised compacts.

Double heterogeneous geometry HTR3 is an exact GT-MHR description which involves the HTR2 geometry as above but now includes also the fuel and erbium compacts made of ceramic-coated fuel and erbium particles within a graphite matrix as it is presented in Fig. 4. Each fuel compact contains 6050 particles and there are 150 compacts along one fuel channel. Similarly erbium particles are placed in the burn-able poison channels. To preserve a corresponding erbium mass, the particles in each compact are organised as dense as possible (12050 particles per compact and 20 compacts per channel). We note separately that in all three cases (HTR1, HTR2 and HTR3) total mass of the materials taken in total and separately was preserved (also see Tables I-II).
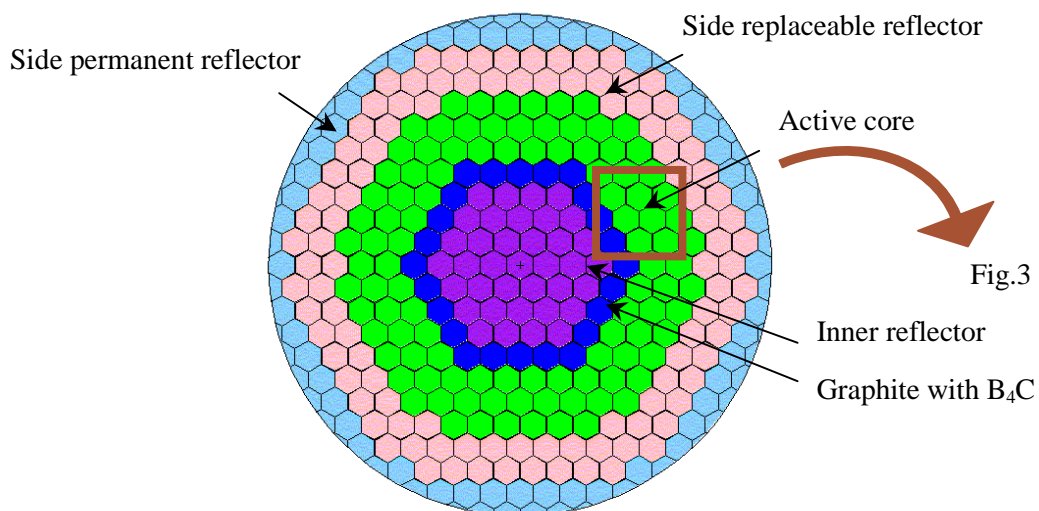


**Figure 2:** A cross section of the GT-MHR homogeneous core with hexagonal structure (HTR1).

Fig. 4

**(A)**　　　　　　　　　　　　　　　　**(B)**
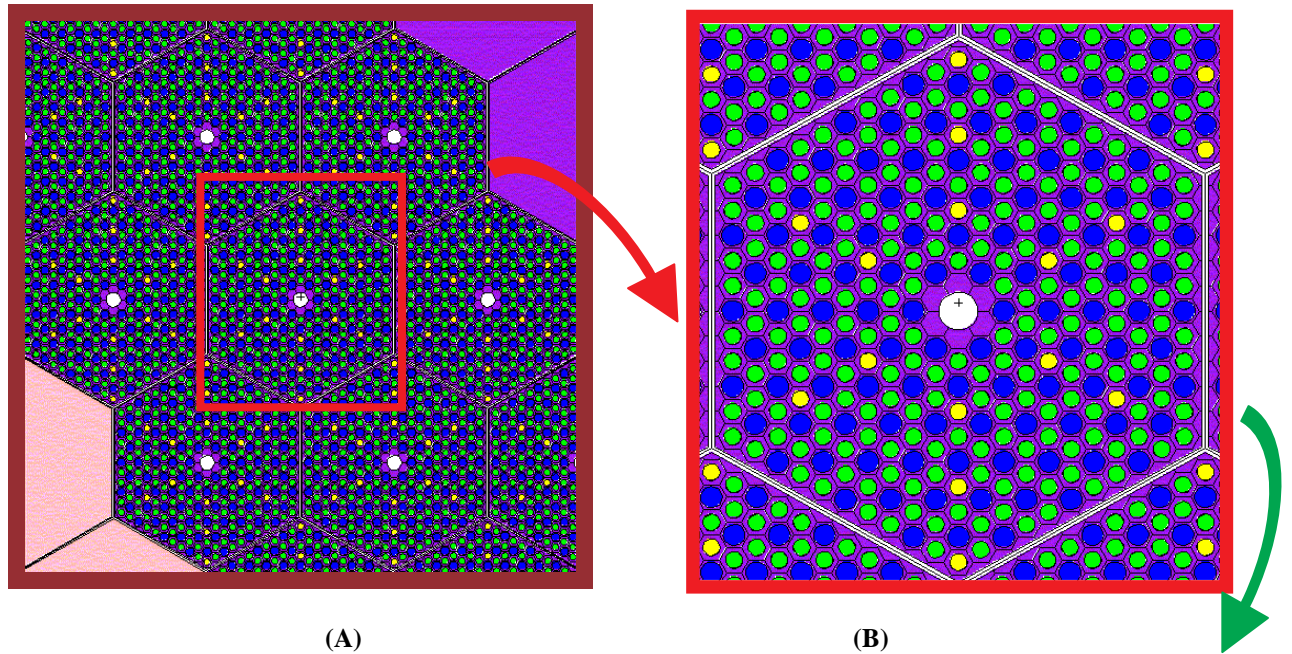
**Figure 3:** Fragments of single-heterogeneous GT-MHR (HTR2): **A)** an active core structure: three rings of hexagonal fuel columns; **B)** magnified view of a separate fuel assembly. Fuel compacts are presented in green, burn-able poison compacts – in yellow. Blue holes stand for He channels, while the remaining violet colour represents the graphite matrix.



310μm

200μm

**(A)**　　　　　　　　　　　　　　　　**(B)**
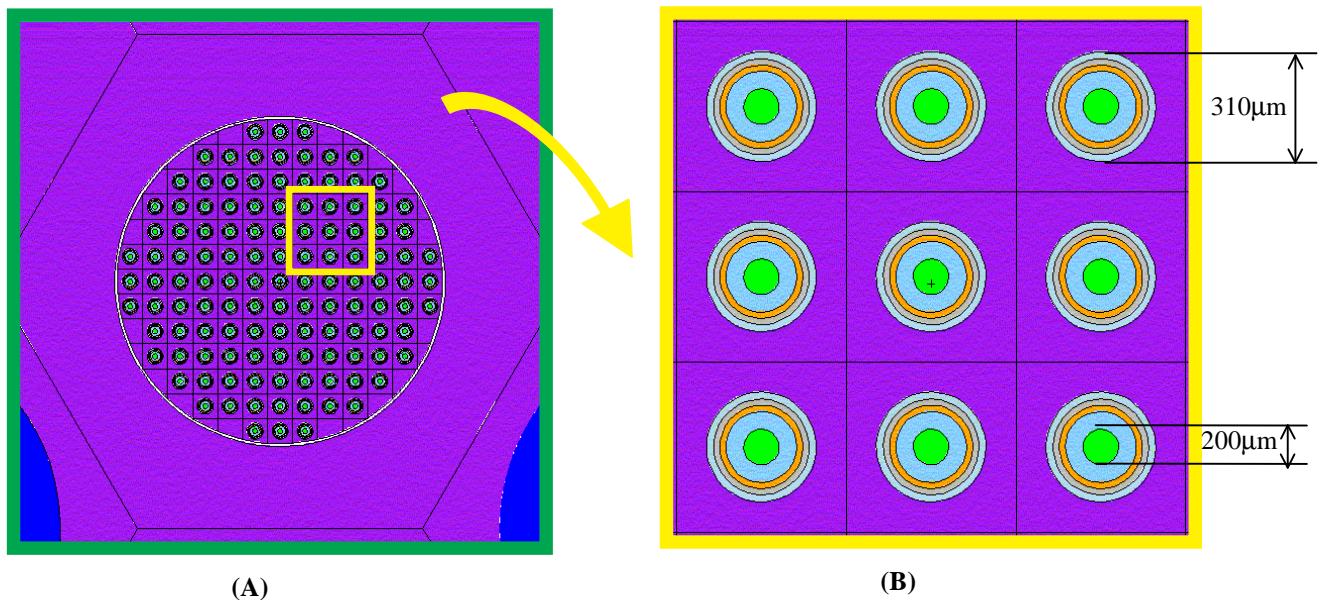
**Figure 4:** Fragments of double-heterogeneous GT-MHR (HTR3): **A)** fuel element (compact) cross section with coated fuel particles; **B)** magnified view of coated fuel particles: spherical kernels of $PuO_{2-x}$ (in green) are surrounded by protective coatings made of $PyC_{buffer}$, PyC I, SiC and PyC II correspondingly. The same structure is valid for particles containing burn-able poison - natural $Er_2O_3$.

The main parameters used for modelling of the three reactor geometry designs are summarised in Table I. Note that in all cases the same fuel-reflector-poison masses were kept. The initial fuel and

burn-able poison composition is presented in Table II. In the case of military plutonium the following isotopic vector was taken: 94.0 % of $^{239}$Pu, 5.4 % of $^{240}$Pu and 0.6 % of $^{241}$Pu (see Table II for details).

**Table I:** Basic GT-MHR parameters.

| | |
|---|---|
| Power, MW$_{th}$ | 600 |
| Active core size:<br>- height, cm<br>- area, m$^2$ | 800.0<br>11.5 |
| Active core volume, m$^3$: | 91.9 |
| Graphite mass in reactor, t: | 616.3 |
| Averaged temperature, $^{o}$C:<br>- active core<br>- inner reflector<br>- side, top and bottom reflectors | 800<br>730<br>500 |

**Table II:** Major GT-MHR material compositions.

| Material | Military Pu |
|---|---|
| Isotopic fuel composition, kg :<br>    $^{238}$Pu<br>    $^{239}$Pu<br>    $^{240}$Pu<br>    $^{241}$Pu<br>    $^{242}$Pu | -<br>659.0<br>37.8<br>4.2<br>- |
| Total plutonium, kg : | 701.0 |
| Isotopic burn-able poison composition, kg :<br>    $^{166}$Er<br>    $^{167}$Er<br>    $^{170}$Er | 138.0<br>94.2<br>61.4 |
| Total erbium, kg : | 293.6 |

## 3.2. k$_{eff}$ and BURNUP RESULTS

We use the same Monteburns code **[3]** in all three cases. ENDF data library (as the most often employed with MCNP) was used for the fuel and structure materials, JENDL data files (having a biggest number of fission fragments) were employed for fission products. We performed our calculations in terms of the once-through fuel cycle scenario at a constant power of 600MW$_{th}$. The length of the fuel cycle is determined according to the following criterion: k$_{eff} \geq 1$.

Fig. 5 presents the behaviour of $k_{eff}$ as a function of time (consequently, as a function of burn-up). In the case of HTR1 $k_{eff}$ drops below 1 approximately after 850 days, while for HTR2 the fuel cycle is somewhat shorter (~800 days). We note that the biggest difference appears in the case of HTR3 - fuel cycle length is only ~550 days. The dependence of $k_{eff}$ significantly differs for all three geometry configurations already at the beginning, namely $k_{eff} = 0.994$, 1.116, and 1.135 for HTR1, HTR2 and
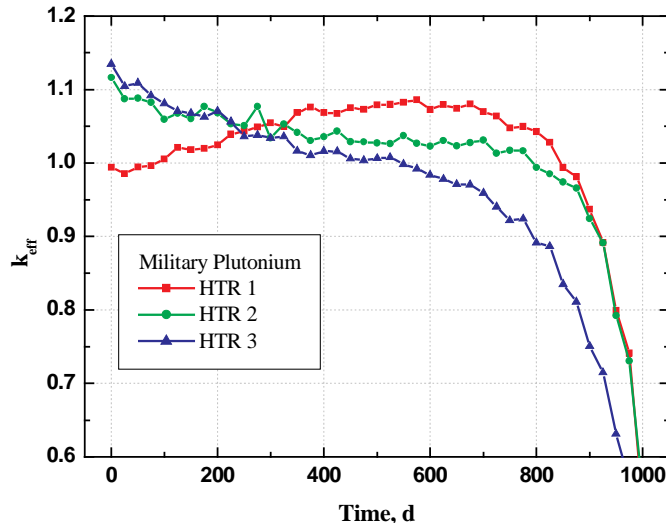
**Figure 5:** A behaviour of $k_{eff}$ for different GT-MHR modelling cases with military plutonium fuel.

HTR3 (with $1\sigma = 0.005$ in all cases). In addition, the $k_{eff}$ curve of HTR1 initially increases and decreases later on as a function of burn-up as shown in Fig. 5. Contrary, for HTR2 and HTR3 the corresponding behaviour of $k_{eff}$ is continuously decreasing. In addition, the $k_{eff}$ curve of HTR3 decreases faster than in the case of HTR2. The major difference between HTR1 and the other two cases can be explained by different consumption of burn-able poison – erbium as shown in Fig. 6. It is clearly seen that erbium is burned much faster in the case of a homogeneous geometry-material specification.
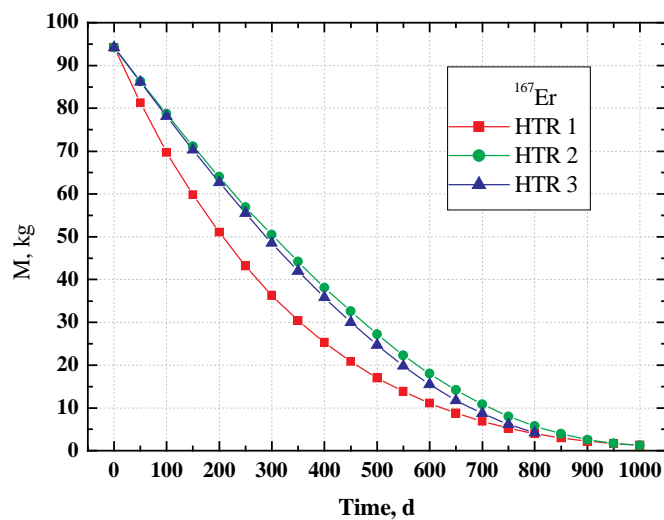
**Figure 6:** Burn-up of $^{167}$Er as a function of irradiation in the case of HTR1, HTR2 and HTR3.

(6)

To explain the above situation one needs to remember the way all three geometries were modelled. In the case of HTR2 and HTR3 Er and Pu are burned in different neutron fluxes since these materials are in different cells: in compacts for HTR2 and in coated particles for HTR3. Contrary, in the case of HTR1 both Er and Pu are irradiated in the same neutron environment defined by the same geometrical cells - hexagons. Mainly for this reason in Fig. 7 for comparison we present averaged neutron fluxes for all geometries considered both in the beginning and at the end of irradiation. Neutron fluxes
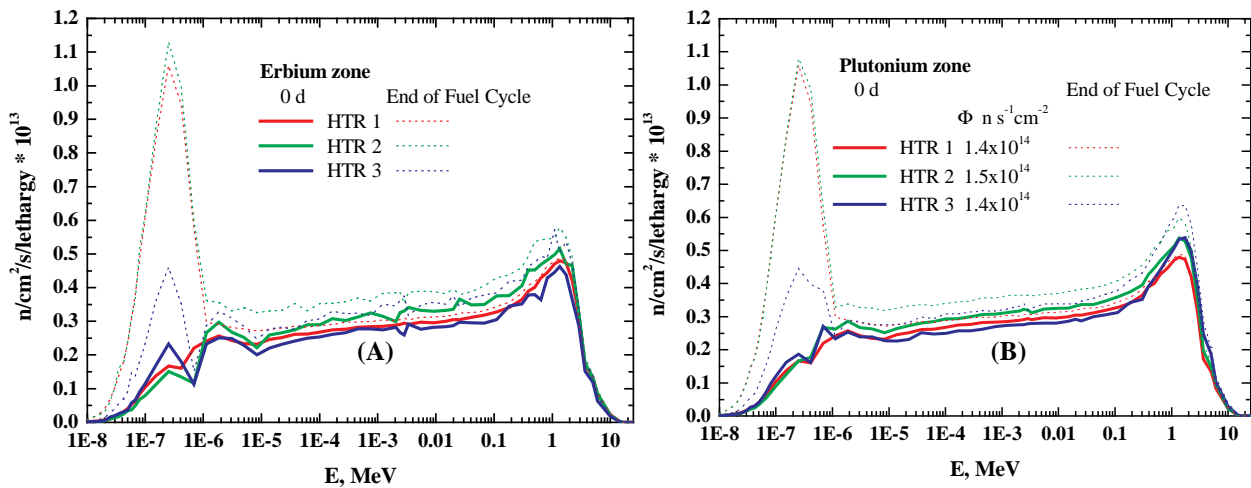


**Figure 7: A)** Neutron flux spectrum in burn-able poison cells for different GT-MHR modelling cases at the beginning and at the end of the fuel cycle. **B)** Same as in A but in the fuel material cells.

"seen" by Er and Pu are presented in separate graphs on the left (8A) and on the right (8B) respectively. We note that for the burn-able poison zone the biggest difference in neutron spectra is in the thermal neutron region (0.5-1.0 eV), where neutrons are suppressed by the presence of Er in high concentration (compare red curve with blue or green). After 800 days of operation the thermal neutron contribution is nearly the same for HTR2 and HTR1 due to the disappearance of the same [167]Er. This is not the case for HTR3 since its fuel cycle ends already after 550 days and Er is not fully consumed by this time. Consequently, much less thermal neutrons are present in this case. It is worth recalling that for HTR2 Er is located in a few particularly positioned cylinders – compacts (see yellow circles in Fig. 3B) and for HTR3 Er -- in 278μm diameter fuel kernels (see yellow circles in Fig. 4B), while for HTR1 Er is distributed all over the active zone of the core (see Fig. 2). This effect naturally makes some influence on the averaged one group cross sections. Indeed, as it is shown explicitly in Table III, for HTR1 the average neutron capture cross section of Er is much higher than for HTR2 and HTR3, while for those two it is comparable.

We should note separately that the neutron spectra in the cells containing fuel are rather similar as shown in Fig. 7B. Contrary to the [167]Er capture cross section, the [239]Pu fission cross sections are also rather similar for all geometries considered (see Table III). Nevertheless, small differences are observed due to the resonance capture of [239]Pu at ~0.5 eV and [240]Pu at ~1 eV in particular. On the other hand, these small differences are somewhat compensated by different flux intensities since in all cases the same constant thermal power is requested (see Fig. 7B). For this reason a corresponding evolution of [239]Pu is also very similar as shown explicitly in Fig. 8.

The biggest difference in fuel evolution is observed in $^{240}$Pu and consequently in $^{241}$Pu. This phenomenon is explained by the self shielding effect, which is enhanced in the case of the HTR3 geometry modelling with microscopic fuel particles. The average capture cross section of $^{240}$Pu in this case is the lowest one compared to the ones of HTR1 and HTR2 (see Fig. 9B), what gives the
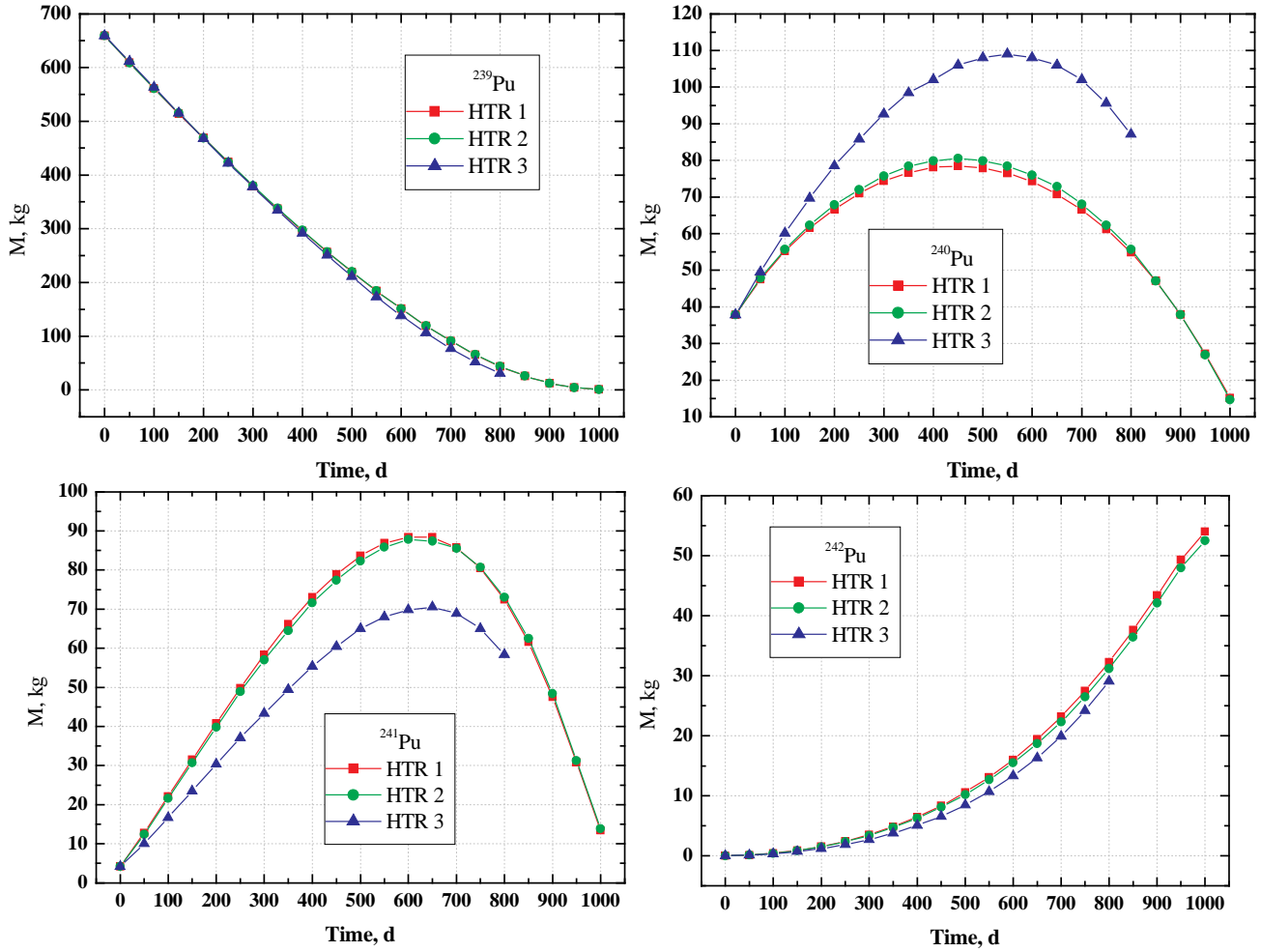


lowest $^{240}$Pu

**Figure 8**: Evolution of mass of Pu isotopes for different GT-MHR geometry configurations.

**Table III:** Effective capture and fission cross sections for different GT-MHR geometry configurations.

| Element | $^{167}$Er $\sigma_c$, barns | | | $^{239}$Pu $\sigma_f$, barns | | |
|---------|------|------|------|------|------|------|
| Time, d | HTR1 | HTR2 | HTR3 | HTR1 | HTR2 | HTR3 |
| 0 | 252 | 145 | 164 | 77.7 | 72.6 | 78.3 |
| 200 | 284 | 172 | 201 | 95.6 | 85.6 | 92.7 |
| 400 | 338 | 227 | 258 | 131 | 111 | 119 |
| 600 | 416 | 320 | 368 | 188 | 159 | 178 |
| 800 | 563 | 493 | 578 | 305 | 267 | 308 |

**(A)**

**(B)**
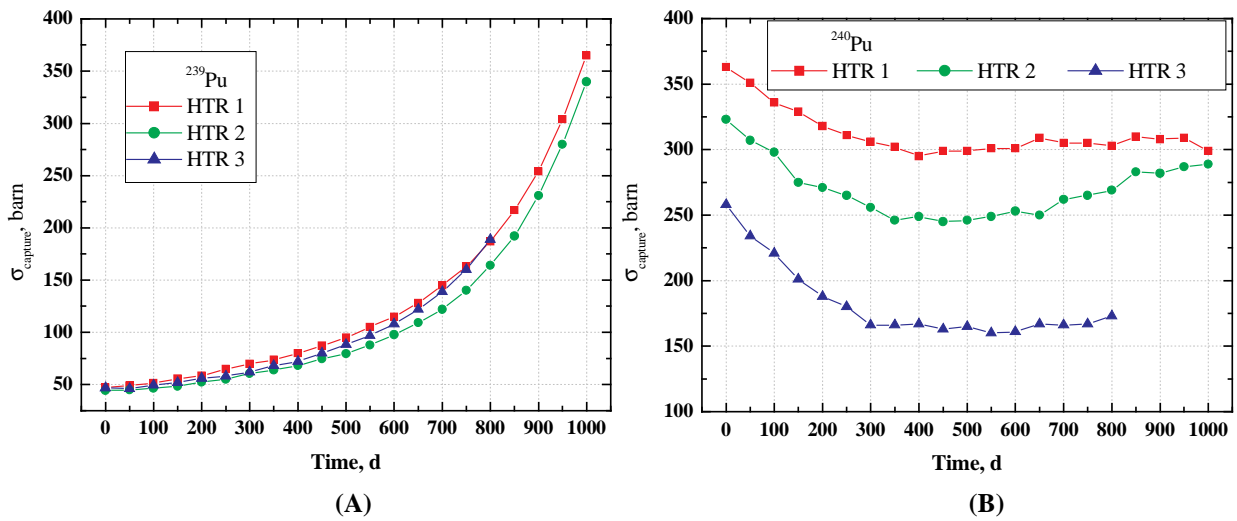
**Figure 9**: **A)** $^{239}$Pu capture cross sections for different GT-MHR geometry configurations  **B)** same as A) but for $^{240}$Pu .

consumption speed. Consequently, in this case the lowest mass of $^{241}$Pu is observed (see Fig. 8). As a matter of fact, this difference, in addition  to the different evolution of Er, strongly influences the behaviour of $k_{eff}$. It is also responsible for the length of the fuel cycle (the shortest in the case of HTR3).

To cross check this self-shielding effect we sliced the micro particle kernel into two separate zones of the same volume. In this way we could clearly observe that the capture cross section of $^{240}$Pu was by ~60 barns higher in the outside  layer compared to the inside layer, where no resonance neutrons were left. Finally, the averaged cross section through the entire particle volume   (it is shown in Fig. 9B) was just in between two partial cross sections.  In our opinion, this observed dependence is a clear warning for civil Pu based fuel cycles, where the percentage of $^{240}$Pu  is much bigger if compared to the military plutonium case. With higher $^{240}$Pu concentration the self-shielding effect as above may be even bigger and more important for the performance of the system.

Finally Table IV summarises the fuel and Er isotopic composition at the beginning and at the end of the fuel cycle. We note that in the case of HTR3 much lower neutron fluence is obtained due to a shorter fuel cycle. Therefore, in some sense the burnup results cannot be compared directly. It is interesting  to note, however, that the evolution of fuel  in the case of HTR1 and HTR2, even though characterized by a completely different behaviour of $k_{eff}$ as already discussed above, is very similar.

**Table IV:** The fuel and Er isotopic composition at the beginning and at the end of the fuel cycle.

| Reactor geometry | | HTR1 | HTR2 | HTR3 |
|---|---|---|---|---|
| Time, days | 0 | 800 | | 550 |
| Fluence, n/cm$^2$ | | $1.10\times10^{22}$ | $1.26\times10^{22}$ | $8.08\times10^{21}$ |
| Actinides | | Mass, kg | | |
| $^{238}$Pu | 0.0 | 1.3 | 1.3 | 0.3 |

(9)

| | | | | |
|---|---|---|---|---|
| $^{239}$Pu | 659.0 | 43.5 | 43.8 | 173.0 |
| $^{240}$Pu | 37.8 | 54.9 | 55.7 | 109.0 |
| $^{241}$Pu | 4.2 | 72.4 | 73.0 | 68.0 |
| $^{242}$Pu | 0.0 | 32.3 | 31.2 | 10.7 |
| $^{241}$Am | 0.0 | 2.6 | 2.5 | 1.8 |
| $^{242}$Am | 0.0 | <0.5 | <0.5 | <0.5 |
| $^{243}$Am | 0.0 | 4.3 | 4.6 | 1.2 |
| $^{242}$Cm | 0.0 | 1.6 | 1.6 | 0.5 |
| $^{243}$Cm | 0.0 | <0.5 | <0.5 | 0.0 |
| $^{244}$Cm | 0.0 | 1.5 | 1.9 | <0.5 |
| $^{245}$Cm | 0.0 | <0.5 | <0.5 | 0.0 |
| Total | 701.0 | 215.0 | 216.0 | 364.4 |
| Burnable poison | Mass, kg | | | |
| $^{167}$Er | 94.2 | 4.0 | 5.7 | 19.8 |

## 4. CONCLUSIONS

A critical GT-MHR dedicated to burn Pu isotopes in the once-through fuel cycle was studied by comparing its performance parameters as a function of different geometry descriptions: homogeneous HTR1, single-heterogeneous HTR2 and double-heterogeneous HTR3. We have shown that it is very important to model the reactor geometry as precise as possible in order to characterise properly the performance of the system (e.g., $k_{eff}$, its behaviour with time, the length of the fuel cycle, burn-up, etc.). The following conclusions are drawn:

1. A significant difference was found in $k_{eff}$ values between HTR1, HTR2 and HTR3 both at the beginning of the fuel cycle as well as in its evolution as a function of burn-up. $k_{eff}$ of HTR2 and HTR3 starts at higher values and it decreases constantly. Contrary, $k_{eff}$ of HTR1 begins at much lower value, increases to its maximum and later decreases. In addition, HTR3 fuel cycle ends much faster compared to the other two cases.
2. A different behaviour of $k_{eff}$ is explained by different modelling of burn-able poison (homogeneous versus heterogeneous distribution) and also by an enhanced self-shielding effect in micro particles (single-heterogeneous versus double-heterogeneous geometry). Consequently, the burn-up of erbium and changes in isotopic fuel composition (e.g., $^{240}$Pu and $^{241}$Pu) is rather different during the fuel cycle.
3. An exact modelling of the fuel particles in the compacts (HTR3) in comparison with single-heterogeneous (HTR2) and homogeneous distributions (HTR1) had much smaller influence on neutron spectrum in the corresponding cells than in the case of burn-able poison. This would suggest that the big number of compacts with fuel particles inside "homogenises" the system indirectly. Consequently, the evolution of $^{239}$Pu at a constant reactor power and a comparable neutron fluence is very similar for all three geometry configurations.

Finally we add that a further step using an exact geometry description (HTR3) with Monte Carlo would be to test GT-MHR performance characteristics with different isotopic compositions in the case of plutonium originating from the spent nuclear fuel. The work along these lines is in progress and will be reported elsewhere.

## REFERENCES

1.  "Gas Turbine-Modular Helium Reactor (GT-MHR) Conceptual Design Description Report", No. **910720**, Revision 1, General Atomics, GA Project No.7658, July 1996, San Diego, USA.
2.  C. Rodriguez et al., "The Once-through Helium Cycle for Economical Transmutation in Secure, Clean and Safe Manner", paper 72 in the *Proceedings of the 6th OECD/NEA Information Exchange Meeting on Actinide and Fission Product Partitioning and Transmutation*, Madrid, Spain, 11-13 December 2000.
3.  H. R. Trellue and D.I. Poston, "User's Manual, Version 2.0 for Monteburns, Version 5B", LANL *preprint* **LA-UR-99-4999** (1999); H.R. Trellue, private communication, April 2000.
4.  J.F. Briesmeister, "MCNP - A General Monte Carlo N-Particle Code", Technical Report LA-12625-M, LANL (1997).
5.  RSIC Computer Code Collection, "ORIGEN 2.1 - Isotope Generation and Depletion Code Matrix Exponential Method", RSIC report CCC-371 (1991).
6.  D. Ridikas et al., "On the Fuel Cycle and Neutron Fluxes of the High Flux Reactor at ILL Grenoble", *Proceedings of the 5th Int. Specialists Meeting SATIF-5*, OECD/NEA, Paris, France, 17-21 July 2000.
7.  D. Ridikas and R. Plukiene, "Modelling of HTRs: from Homogeneous to Exact Heterogeneous Core with Monte Carlo", Proceedings of *the Int. Conference PHYSOR 2002,* Seoul, Korea, October 7-10, 2002.
8.  F. Damian, "Capacity Analysis of HTRs in terms of utilisation of fissile materials", CEA Saclay, *report* **CEA-R-5981** (PhD thesis in French) 2001; also see F. Damian *et al.* in Proceedings of *the Int. Conference PHYSOR 2002,* Seoul, Korea, October 7-10, 2002.
9.  D. Ridikas et al., "Critical and Sub-Critical GT-MHRs for Waste Disposal and Proliferation-Resistant Plutonium Fuel Cycles", paper 71 in the *Proceedings of the 6th OECD/NEA Information Exchange Meeting on Actinide and Fission Product Partitioning and Transmutation*, Madrid, Spain, 11-13 December 2000.
10. D. Ridikas et al., "Comparative Analysis of ENDF, JEF and JENDL Data Libraries by Modelling High Temperature Reactors and Plutonium Based Fuel Cycles: Military Pu case", Proceedings of the *Int. Conference on Nuclear Data for Science and Technology (ND2001)*, Tsukuba, Japan, 7-12 October 2001.
11. D. Ridikas et al., "Comparative Analysis of Different Data Libraries for the Performance of High Temperature Reactors (GT-MHR): Civil Pu case",  Proceedings of *the Int. Conference on Accelerator Applications/Accelerator Driven Transmutation Technology and Applications (AccApp/ADTTA'01)*, 12-15 November 2001, Reno, Nevada, USA.